THERMODYNAMIC MODELING OF A CLOSED GAS TURBINE PROCESS WORKING WITH HELIUM AND STOICHIOMETRIC COMBUSTION OF HYDROGEN AND OXYGEN

M. Schatz – M. Wachter

Institute of Thermal Turbomachinery and Machinery Laboratory (ITSM)
University of Stuttgart
Germany

schatz@itsm.uni-stuttgart.de

ABSTRACT

For a successful transition of power generation away from fossil and nuclear fuels to renewable energy sources, the problems related to the storage of temporary surplus solar or wind energy and the subsequent utilization has to be solved. A promising approach for this is the generation of hydrogen from electrolysis, which can then be stored and used when necessary. However, large scale power generation from hydrogen with outputs in the Megawatt-range is currently difficult, as fuel cells do not offer such a large power output both from a technical and economical perspective and firing hydrogen in open cycle gas turbines will inevitably lead to high NOx-emissions, which is detrimental to the environment. This paper presents the results of a theoretical study of a closed cycle gas turbine working with helium and a stoichiometric combustion of hydrogen and oxygen, which is also a product of electrolysis. As helium is an inert gas, it is not affected by the combustion process, hence only water vapour is formed, which can be separated by condensation. As a consequence the process would allow large power outputs at zero emissions. For the study, different thermodynamic processes have been evaluated, starting from a simple closed cycle Brayton process to more sophisticated cycles with intercooling and humidification. For all processes, parameter studies have been performed to assess the sensitivity and impact of different parameters such as pressure ratio or turbine inlet temperature. In order to ensure the validity of the model, component efficiencies deduced from publications on the former Oberhausen II closed cycle helium gas turbine have been used. The results show that already the simple cycle process yields good efficiencies comparable to those of current state-of-the-art gas turbines. The improvement that can be achieved using process variations are considerably higher than for an open loop process, indicating that efficiencies in excess of 50% could be reached.

KEYWORDS

CLOSED CYCLE GAS TURBINE, PROCESS MODELING, CYCLE EFFICIENCY

NOMENCLATURE

Symbols

c_p	Specific heat capacity [kJ/kgK]	p	Pressure [Pa], [bar]
H	Enthalpy [kJ/kg$_{He}$]	q	Specific heat [kJ/kg$_{He}$]
h_f	Formation Enthalpy [kJ/mol]	T	Temperature [K], [°C]
M	Mass [kg]	w_t	Specific work [kJ/kg$_{He}$]
M	Molar mass [kg/mol]	x	Molar fraction [-]

Greek symbols

ε	Rel. pressure loss [%]	φ	Rel. humidity [%]
γ	Isentropic exponent [-]	π	Pressure ratio [%]
η	Efficiency [-]		

Subscripts and abbreviations

C	Compressor	id	Ideal
Comb	Combustor	in	At the inlet
Con	Condenser	l	Liquid phase
eff	Effective	LP	Low Pressure
G	Gaseous phase	max	Maximum
H_2O	Water or water vapor	out	At the outlet
He	Helium	Rec	Recuperator
HEX	Heat Exchanger	T	Turbine
HP	High Pressure	TIT	Turbine Inlet Temperature
Hum	Humidificator	TTD	Terminal Temperature Difference

INTRODUCTION

In the light of an ever increasing global demand for energy together with the foreseeable decline of fossil fuels as well as the threat of global warming due to excessive worldwide CO_2-emissions, a change towards renewable sources of energy is inevitable. However, a major problem of power generation from renewables, such as wind and solar, is their volatility. Thus, excessive power generated during periods of abundant energy (i.e. during the day or in windy seasons) must be stored for those times where consumption exceeds the available supply. One approach to solve this challenge is known as “Power to Gas” and includes the generation of hydrogen using electrolysis. To date, the storage of hydrogen itself is a difficult task, requiring high pressures of up to 700 bar or even liquefaction, both being very energy intensive. Therefore, “Power to Gas” often includes the generation of methane from hydrogen, a process that circumvents the hydrogen storage problem, yet at high energy input and correspondingly lower efficiencies. Recently however, the chemical storage of hydrogen using so-called LOHCs (Liquid Organic Hydrogen Carriers), such as Carbazole, is opening completely new pathways and an extremely simplified storage and handling (Teichmann et al., 2011).

Another aspect of hydrogen-based energy economics is the actual power generation from hydrogen. Up to now, the focus for this is mainly on fuel cells, however, a cost effective and flexible generation of power in the Megawatt- or even Gigawatt-range based on fuel cells is not conceivable in the near future. These demands are all met by power plants that use thermal turbomachines such as steam turbines or gas turbines and efforts are currently being made to develop gas turbine combustors that can operate on fuels with high hydrogen content. This approach is also not free from disadvantages, as the combustion of hydrogen in air results in excessive NO_X-formation.

In order to avoid the problem of NO_X-formation inherent to the combustion of hydrogen in air, the work presented here focuses on a closed-cycle gas turbine process with stoichiometric combustion of hydrogen and oxygen – both products of electrolysis – in an inert working fluid. In this process, only water vapor is formed during combustion, which can be removed from the cycle by means of condensation, thus resulting in a completely emission-free process. Helium has been chosen as working fluid for this study because of its beneficial properties and also because some closed-cycle gas turbine plants operated with helium have already been built and operated in the past.

Apart from the basic Brayton-process, a number of process variations have been investigated in order to increase the overall efficiency. These include different methods of adding water vapor for the purpose of intercooling and increasing the turbine mass flow.

Closed-cycle gas turbines operated with helium

The concept of closed-cycle gas turbines is basically as old as that of their open cycle counterparts. The first experimental closed-cycle gas turbine power plant with a power output of 2 MW and an efficiency of 31.6 % went into service already in 1939. Until 1981, 24 experimental and commercial facilities have been built for power generation, air separation or research purposes. For an overview of all facilities built, the interested reader is referred to Frutschi (2005)

The main advantages of closed-cycle gas turbines are twofold. First of all, the process can be run at an elevated pressure level which results in a reduced plant size for a given output. In addition, the plant load can easily be adjusted by changing the pressure level using inventory control. This allows to reduce the mass flow within the cycle (and hence the power output) while the volume flows within the system and consequently the velocity triangles for the turbomachinery stages are maintained, thus only minor changes of turbomachinery efficiencies occur.

However, closed cycle gas turbines suffer from comparably low turbine inlet temperatures, as heat addition is performed via large gas heaters for which the upper temperature limit is generally in the range of less than 700°C, i.e. comparable to modern steam turbine facilities. Apart from the huge expenses for such gas heaters, the thermal efficiencies of simple conventional open-cycle gas turbine power plants with much higher turbine inlet temperatures exceed that obtained for closed-cycle facilities so that the latter suffer from an economic disadvantage. Using stoichiometric combustion of hydrogen and oxygen could solve this problem, as the turbine inlet temperature level can be increased to that of open-cycle gas turbines using cost effective and compact combustors instead of large gas heaters. The water vapor generated can be removed from the process by means of condensation.

With this approach, a further degree of freedom emerges, as the working fluid can be chosen independently. From thermodynamics, it is well known that the efficiency of the ideal Brayton-cycle is a function of pressure ratio and isentropic exponent of the working fluid.

$$\eta_{id} = 1 - \pi^{-(\gamma-1/\gamma)} \tag{1}$$

Thus, helium with $\gamma = 1.66$ has an inherent advantage with regard to efficiency compared to basically all other gases for elevated temperatures. In addition, helium also has a high specific heat capacity and hence superior heat transport and heat transfer properties. On the other hand, the said thermodynamic properties render helium compression based on turbomachinery challenging. As a consequence, the achievable stage pressure ratio is generally quite low (Yan et al, 2008).

THERMODYNAMIC MODELING

All system components are modelled individually as subsystems in MATLAB/Simulink with input and output interfaces for the boundary conditions and thermodynamic state variables. These subsystems are then arranged to form the respective cycle process under consideration. Because the mass flow changes considerably within the process due to the addition of water vapor in the course of combustion or during intercooling by means of humidification as well as due to condensation, the various specific works and heats are related to 1 kg of helium, as the mass flow of the latter is constant. The following assumptions and simplifications have been made for the process:

- Ideal working fluid
- Changes of kinetic and elevation energy are neglected
- Complete stoichiometric combustion
- Adiabatic components except for heat exchangers
- Potential cooling flows in the first stages of the turbine are not considered

Properties of helium and water

Due to its biatomic nature, helium can generally be assumed to be a perfect gas with a constant specific heat capacity of $c_{p,He} = 5.193$ kJ/kg K (McCarty, 1973). To model the thermodynamic properties of water vapor, the so-called NASA-polynomial is used (McBride, 1993), whereby different coefficients are used for a temperature range of less or more than 1000 K. A constant specific heat of $c_{p,H20(l)} = 4.182$ kJ/kg K has been set for liquid water because of the minor dependency of specific heat on pressure and temperature. For the calculation of the saturation pressure of water vapor, the Wagner-equation is used (Wagner, 1973); the specific enthalpy at the boiling point is calculated using a 4th-order polynomial based on tabulated values from (VDI, 2006). As the working fluid used is actually not pure helium but rather a mixture of helium and water vapor at all instances of the process, the mixture properties are calculated based on the respective mass fractions. Therefore, significant changes of fluid properties occur throughout the processes.

Component models

Combustion chamber

The chemical reaction occurring in the combustor is described by the following equation:

$$y\ mol\ He + z\ mol\ H_2O + 2\ mol\ H_2 + 1\ mol\ O_2\ \rightarrow y\ mol\ He + (z+2)\ mol\ H_2O \qquad (2)$$

Note that the water vapor on the left hand side of equation (2) accounts for residual gas that has not been removed in the heat exchanger (condenser) upstream of the compressor. For the combustor modeling, the temperature at the outlet (i.e. at the turbine inlet) is imposed as a boundary condition. The amount of helium necessary to obtain the given outlet temperature is determined using the first law of thermodynamics. This results in

$$\textstyle\sum_{Products} n_i h_{f,i} - \sum_{Reactands} n_i h_{f,i} = 0 \qquad (3)$$

Combining equations (2) and (3), the molar quantity of helium can be calculated based on the enthalpies of formation h_f as

$$y = \frac{1\ mol_{O_2} \cdot h_{f,O_2}^{T_{O_2};p_{in}} + 2\ mol_{H_2} \cdot h_{f,H_2}^{T_{H_2};p_{in}} - 2\ mol \cdot h_{f,H_2O}^{T_{out};p_{H_2O,out}}}{h_{f,He}^{T_{out};p_{He,out}} - h_{f,He}^{T_{in};p_{He,in}} + \frac{x_{H_2O,in}}{1-x_{H_2O,in}} \cdot \left(h_{f,H_2O}^{T_{out};p_{H_2O,out}} - h_{f,H_2O}^{T_{in};p_{H_2O,in}}\right)} \qquad (4)$$

Compressor and Turbine

For both turbomachinery components, pressure ratio, inlet temperature and inlet mass fractions of helium and water vapor are imposed as boundary conditions. Moreover, the polytropic efficiencies are set. In order to calculate the respective outlet temperatures from the polytropic relation, a recursive loop is performed, where both outlet temperature and resulting average specific heat capacity are calculated until the deviation between two subsequent iterations is below 0.1 %. Specific work is then determined using the enthalpy balance between inlet and outlet.

For the cycle calculations the turbine pressure ratio is specified. Thereafter, all pressures within the process are calculated from the imposed compressor outlet pressure, the turbine pressure ratio and the pressure losses set for the different components as described below.

From the turbine and compressor performance calculations the net specific work output can be calculated. The specific heat input during combustion is determined from the lower heating value of hydrogen and the mass ratio of helium and hydrogen from equation (2) and equation (4). With these parameters, the overall thermal efficiency is calculated as follows:

$$\eta_{therm} = \frac{|w_{t,net}|}{q_{Comb}} = |w_{t,net}|\ \frac{m_{He}}{m_{H_2} LHV_{H_2}} = |w_{t,net}|\ \frac{y M_{He}}{2 M_{H_2} LHV_{H_2}} \qquad (5)$$

Heat exchangers and humidifiers

All heat exchangers are modeled based on heat exchanger efficiency which is defined as

$$\eta_{HEX} = \frac{\Delta h_{eff}}{\Delta h_{max}} \tag{6}$$

Δh_{eff} is the enthalpy change across the heat exchanger for the actual fluid stream of interest, while Δh_{max} is the enthalpy difference that would be achieved if the minimum temperature of the cooling fluid was achieved. For the calculation of temperatures from enthalpies, again a recursive procedure to compute both specific heat capacity and temperature is implemented. For the heat exchanger and condenser placed upstream of the compressor, the amount of liquid water condensed is determined based on the calculation of the saturated state at the cooler outlet. The cooling water mass flow is not restricted in this study, hence the state and composition of the fluid is a function of the HEX efficiency and hence condenser outlet temperature, which varies between 27°C and 43°C for all operating points considered here. Condensation is only allowed in the condenser; if condensation occurs at another heat exchanger, such as the recuperator or the economizer, the calculation is interrupted.

Humidifiers are modelled as enthalpy mixers, whereby the humidity at the outlet as well as a pressure drop is specified. When humidification is used, the pump and the corresponding work input are also taken into account. For a conservative estimate, it is assumed that complete saturation will not be achieved in the humidifiers and a relative humidity of 80 % is set.

Every heat exchanger features a pressure drop. Moreover, piping pressure losses are specified for every connection between the various components. It has to be mentioned, though, that the compression of hydrogen and oxygen has not been taken into account for the present study, as there is a wide range of operating pressures for state-of-the-art electrolysers.

Table 1: Boundary conditions and modeling assumptions for the present work

Parameter	Value	Remarks
Turbine inlet temperature $T_{T,in}$	900/1500 °C	
Turbine pressure ratio π_T	2 – 10	Increments of 0.5
Cooling water temperature T_{cool}	25 °C	
Polytropic Turbine efficicency η_T	89%	From Oberhausen II data, avg. efficiency of HP/IP Turbine
Polytropic compressor efficiency η_C	86%	From Oberhausen II data, avg. efficiency of HP/IP Compressor
Recuperator efficiency η_{Rec}	88%	From Oberhausen II data
Condenser efficiency η_{Con}	97%	
Relative pressure loss of combustor ε_{Comb}	3,8%	
Rel. pressure loss of gas cooler/condenser ε_{Con}	1,4%	
Pressure loss recuperator, HP branch $\varepsilon_{Rec,HP}$	1,3%	
Pressure loss recuperator, LP branch $\varepsilon_{Rec,LP}$	1,1%	
Relative pressure loss for piping sections ε_{pipe}	0,3%	Average value from Oberhausen II data
Relative humidity at humidifier outlet $\varphi_{Hum,out}$ (where applicable)	80%	

A detailed description of the whole modeling process would go beyond the scope of this publication. The interested reader is referred to (Wachter, 2018). The boundary conditions and modeling assumptions used for this study are given in Table 1. Component efficiencies and pressure losses have been taken from design data of the Oberhausen II power plant (Frutschi, 2005 and

Bammert et al. 1974), with a projected power output of 50 MW. With regard to the fact that this power plant has been taken into service in 1974, it can be expected that an improvement of component efficiencies could be achieved using current state-of-the-art design methods and hence the overall process efficiency obtained in the current study is considered to be a conservative estimate. For example, compressor polytropic efficiencies exceeding 88 % have already been measured by Yan et al. (2006) for a 4-stage axial helium compressor at a pressure ratio of 1.17.

The thermodynamic model applied for the present study has been validated using the available data for the Oberhausen II power plant. Very good agreement was found between the computational results and the published data as can be seen from Fig. 1. The difference in the net efficiency is due to modeling uncertainties such as gearbox efficiency or heat loss along the piping, which has not been considered for the model.

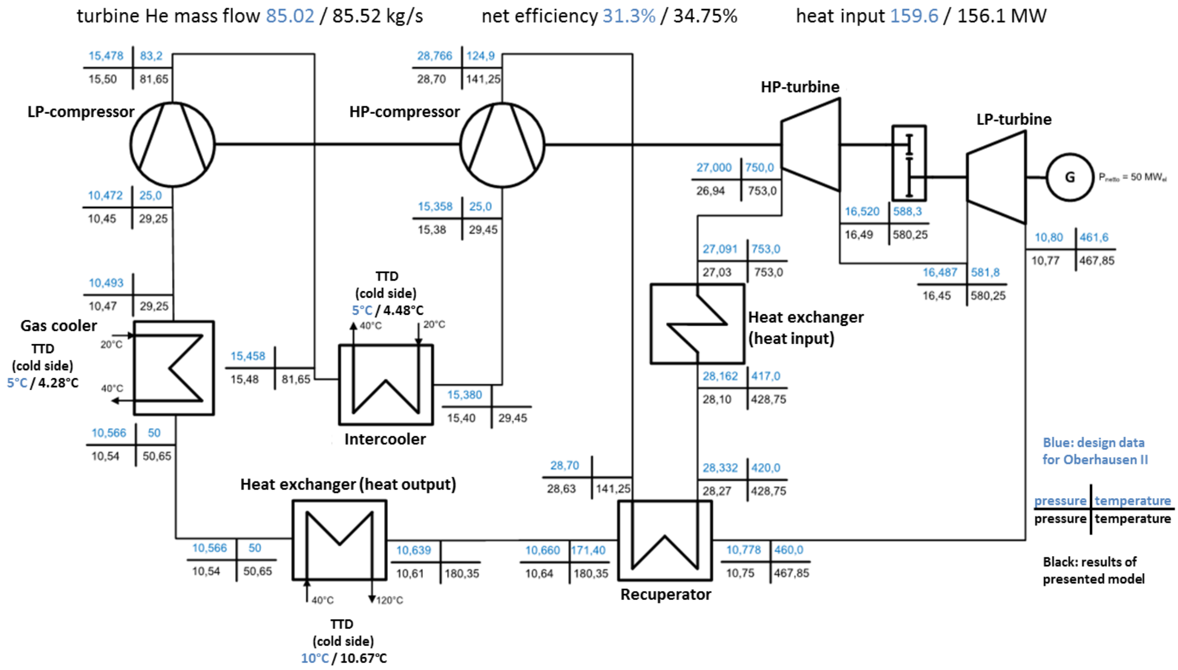

Fig. 1: Comparison of design data for Oberhausen II to results of the presented model

For the current study, turbine inlet temperatures of 900°C and 1500°C have been considered, the first being close to the limit for uncooled turbine blades (e.g. in micro gas turbines), while the latter is achieved for modern large heavy-duty gas turbines featuring sophisticated cooling systems. It has to be mentioned here that cooling mass flows have not been taken into account in the present study. However, for the cycle under consideration, steam would be an ideal cooling fluid and could be generated with relatively low effort.

RESULTS

Base case: closed-cycle recuperated Brayton-process

The block diagram of the base case is shown in Fig. 2. In order to assess the impact of system pressure on the process efficiency, three different pressure levels have been investigated. For this purpose, the compressor outlet pressure (i.e. the highest pressure within the cycle) has been set to 5 bar, 10 bar and 100 bar, respectively. The results of the calculations for the different pressure levels are shown in Fig. 3. Best performance with efficiencies of 34.4 % and 45.5 % at a TIT of 900°C and 1500°C, respectively, is achieved for a system pressure level of 100 bar, whereby the maximum efficiency is obtained at turbine pressure ratios of $\pi_{T,900} \sim 2.5$ and $\pi_{T,1500} \sim 4 - 4.5$. For the lower system pressures of 5 bar and 10 bar, the best performance is about 1.5 – 2 %-points lower at absolute values of 32.6 % and 43.7 % and shifted to slightly higher pressure ratios.

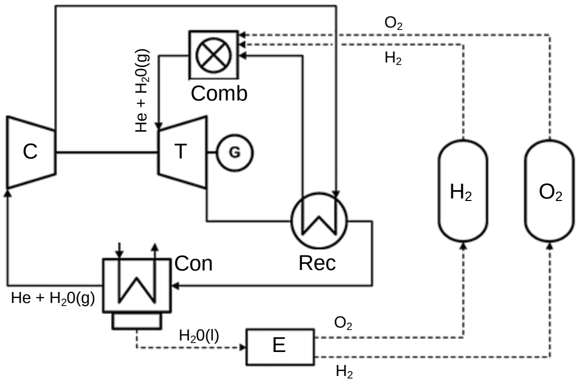

Fig. 2: Block diagram of the base case

The change of performance obtained for the different pressure levels results from the variation of the thermodynamic properties of water and the subsequent impact on the water mass fractions within the system. At a system pressure of 100 bar, the water mass fraction upstream of the compressor as well as at the combustor outlet is lowest as can be seen from the left diagram in Fig. 4. While this causes only a minor change in compressor work (less than 2% compared to a system pressure level of 10 bar), it has a significant impact on the heat input necessary within the combustor to achieve the specified TIT. The reduction of turbine specific work visible in the plot on the right hand side of Fig. 4 is also due to the low water mass fraction and hence lower mass flow per kg of helium. As the decrease of q_{Comb} clearly outweighs the reduced turbine specific work w_{tT}, a system pressure of 100 bar yields superior efficiency, yet at the lowest specific work output. Thus, from the point of efficiency, the higher system pressure level would be most suitable for the process. However, with regard to possible leakage problems – it is known from Oberhausen II that the daily loss of helium at a pressure level of 29 bar was around 0.7 % of the overall inventory, see Bammert et al. (1974) – all following discussions will focus on a pressure level of 10 bar, as this seems to be a more realistic option in terms of operational aspects.

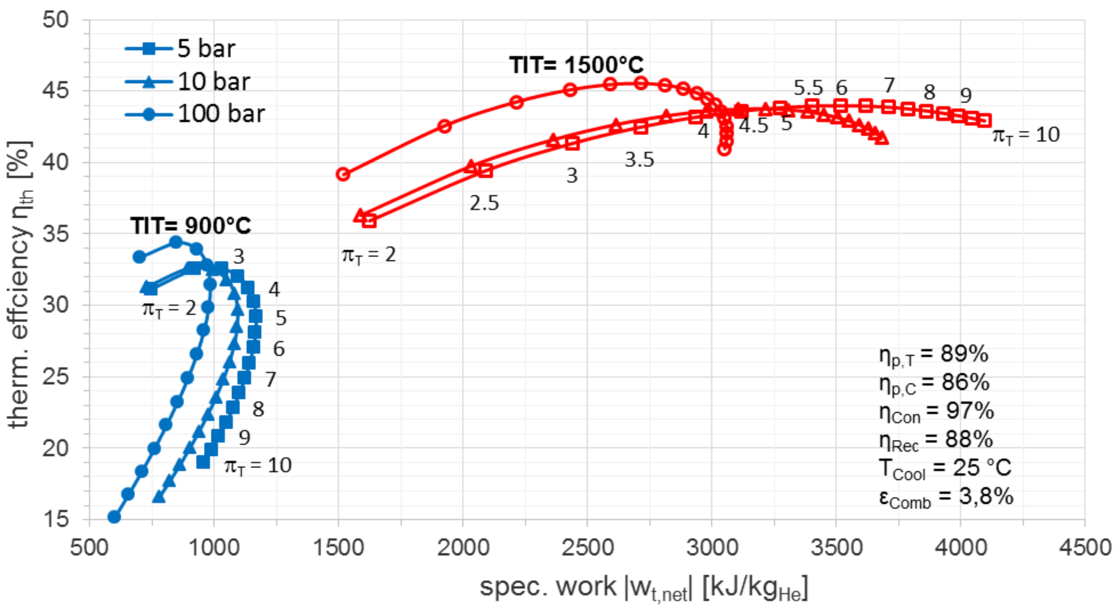

Fig. 3: Thermal efficiency and net specific work output for the base case at turbine inlet temperatures of 900°C and 1500°C at system pressures levels of 5 bar, 10 bar and 100 bar

While the efficiencies calculated for the base cycle are in fact slightly lower as those stated for conventional recuperated air-breathing gas turbines as published e.g. by Boyce (2011), the specific work output of the process with helium is almost one order of magnitude higher. This is visualized in Fig. 6, where the computed efficiencies and specific work output for all processes considered here at a system pressure level of 10 bar are compared to data for recuperated and combined intercooled/recuperated air-breathing processes taken from Boyce (2011). Note that the turbine inlet temperatures are different from those used in the present study. For the lower temperature case, the TIT is 982°C and 871°C for the recuperated and the combined intercooled/recuperated process, respectively. For the high temperature case, the TIT is 1538°C and 1204°C (data at higher TIT was not available for this case). The efficiencies of the standard recuperated air breathing process are 2-3%-points higher than those of the base process considered here at both temperature levels.

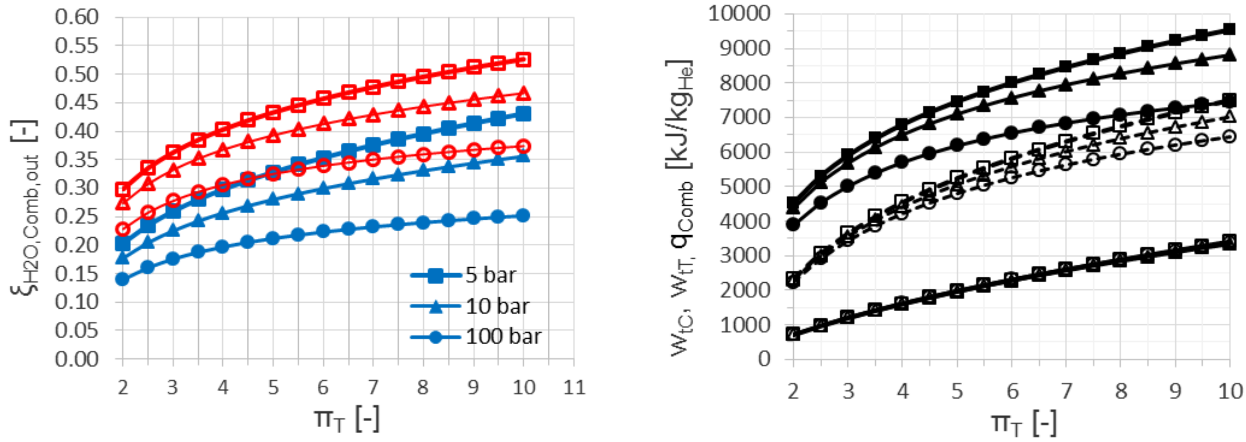

Fig. 4 left: Water vapor mass fraction at the combustor outlet for a TIT of 900° C (blue curves, solid symbols) and 1500° C (red curves, open symbols).
Right: Specific compression work (solid line, open symbols), specific turbine work (dashed line) and combustor specific heat input (solid line, solid symbols) at 1500° C TIT

Process variations

Three process variations have been taken into account for the present work, with the goal to increase both the thermal efficiency and the specific work output of the cycle. The corresponding block diagrams for the process with conventional intercooling, diabatic or evaporative intercooling and humidification are shown in Fig. 5. Results of all process variations studied are compiled in Fig. 7 to Fig. 10.

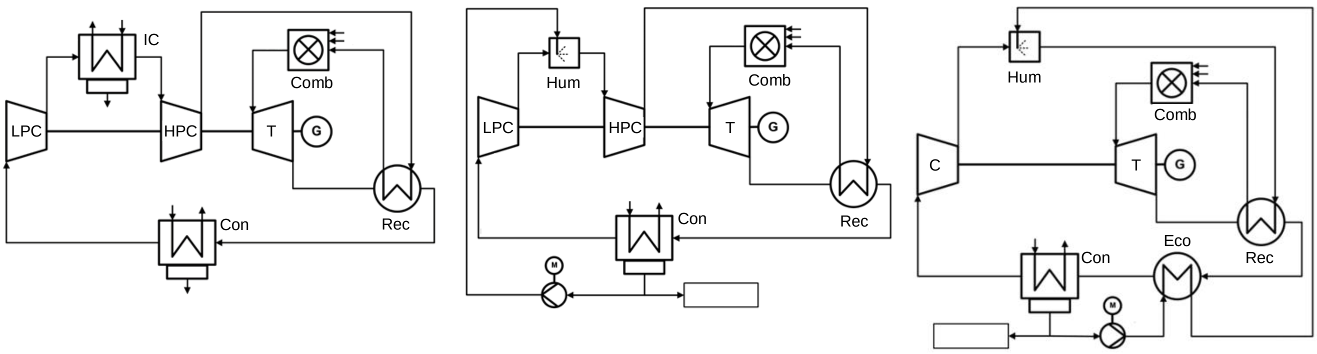

Fig. 5: Block diagrams of process variations investigated for the present work. From left to right: Conventional intercooling, evaporative intercooling and humidification

Process with intercooling

As a first step to improve the system performance, intercooling is modelled. The heat rejection after a first compression process results in a lower high pressure compressor inlet temperature and thus reduced compression work for the second compression, hence overall compression work is reduced. This leads to a significant increase of efficiency and specific work output, which can be seen from Fig. 6. Efficiency increases to 36.7 % and 49.1 % for 900°C and 1500°C TIT, respectively, yet at elevated turbine pressure ratios. A pressure ratio of $\pi_{T,900} \sim 3.5$ can be seen as acceptable with regard to the limited stage pressure ratio feasible for helium and the resulting number of compressor stages, however $\pi_{T,1500} > 7$ would certainly require some ideas with regard to the rotordynamics of the shaft, as the number of compressor stages would accumulate to 40 and beyond. As can be expected, the compression ratio at which intercooling is introduced has an impact on the overall performance. This ratio is expressed using the exponent N with

$$\pi_{LPC} = \pi_C^N$$

For N = 0.5, i.e. $\pi_{LPC} = \pi_{HPC}$, the highest efficiency is achieved for both turbine inlet temperatures studied. Therefore, the discussion of results will be restricted to this ratio.

From Fig. 9, the reduced compression work compared to the base case is evident. At a pressure ratio of 10, the decrease amounts to more than 27 % relative to the base case, despite the fact that the fluid features an increased specific heat capacity (and thus higher isentropic exponent) within the HPC compared to the LPC.

As the high pressure compressor outlet temperature is lower, the heat transfer within the recuperator is considerably enhanced and the turbine exhaust flow temperature downstream of the recuperator decreases. Because of this, more water can be removed in the condenser, which leads to an overall lower water vapor mass fraction within the complete process. In fact, the intercooled process features the lowest water vapor mass fraction of all cycles investigated here, as can be seen from Fig. 8. While this hardly affects the amount of heat added in the combustor (it changes by less than 1 %), it leads to a reduction of specific turbine work as shown in Fig. 9.

For the lower temperature, the maximum efficiency obtained is still about 1%-point lower as that of the air-breathing process with intercooling and recuperation used for comparison. For the higher temperature used, the efficiencies cannot be compared directly, as the air-breathing process used features a considerably lower TIT of 1204°C.

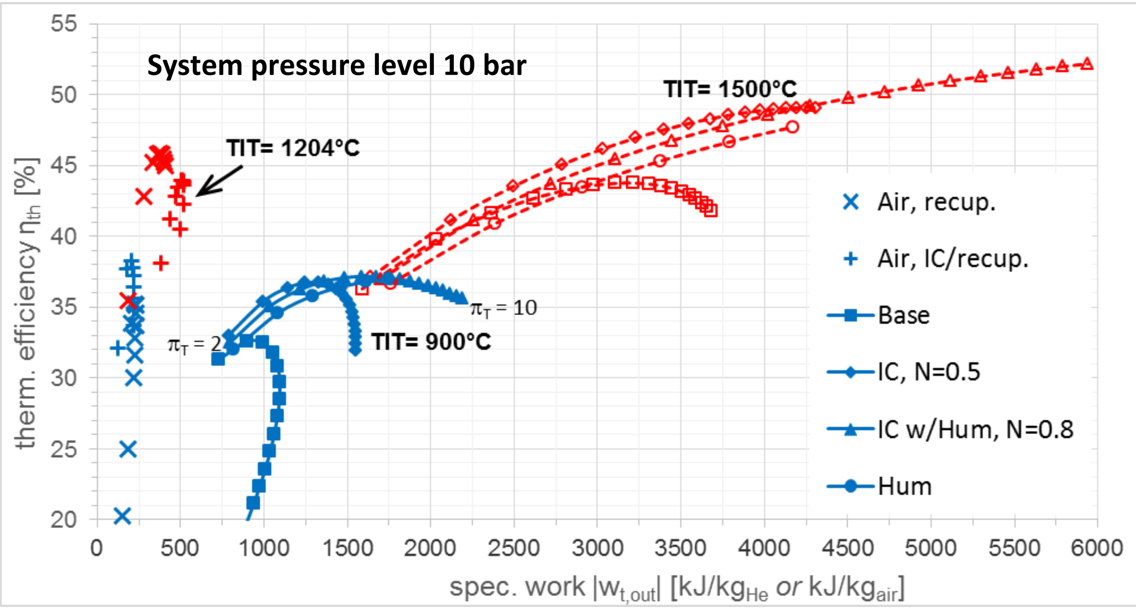

Fig. 6: Thermal efficiency vs. net specific work output for all processes turbine inlet temperatures of 900°C and 1500°C and comparison to data for air-breathing processes taken from Boyce (2011) with TIT's of 982°C / 1538°C (Air, recup.) and 871°C / 1204°C (Air, IC/recup.)

Process with evaporation intercooling

From the results obtained above, the question arises whether diabatic cooling, i.e. evaporation, can bring a benefit in terms of efficiency and specific work output, as the heat introduced in the course of compression is not removed from the process but rather used to increase the overall mass flow within the system. Another effect of humidification and the subsequent enlarged mass fraction of water vapor is the variation of gas properties.

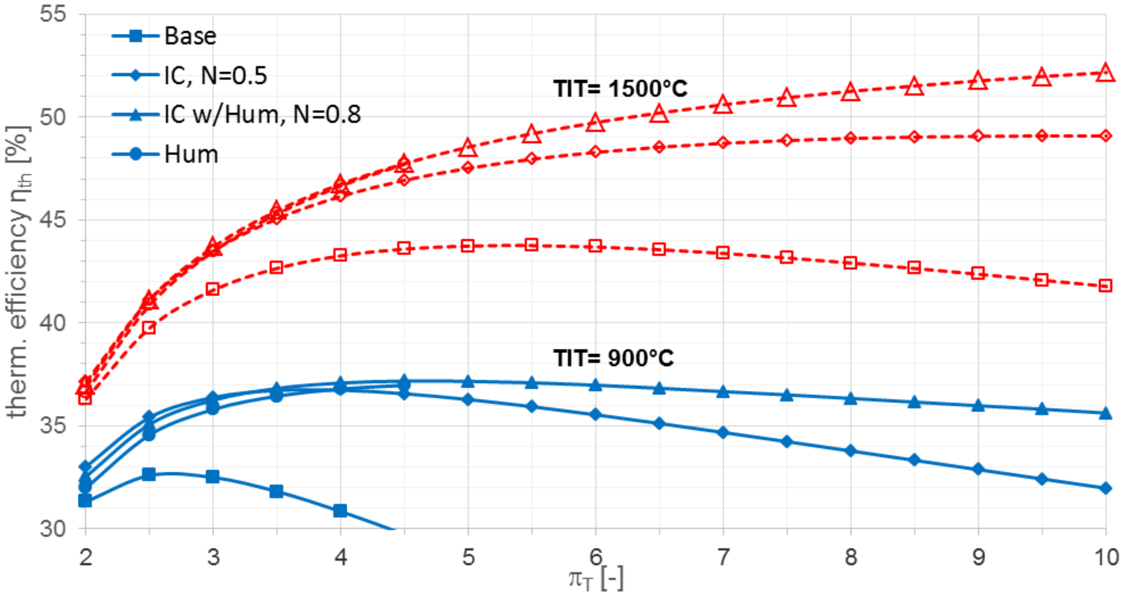

Fig. 7: Thermal efficiency vs. turbine pressure ratio for all processes at turbine inlet temperatures of 900°C and 1500°C

For the second (HP) compression, the isentropic exponent is noticeably decreased as can be seen from Fig. 10, leading to a lower specific work necessary for compression.

At the same time, though, the mass flow for the second compression is also increased, which in turn results in a higher power demand. Moreover, the turbine power output is affected, as the favorable effect caused by the high specific heat capacity of helium in the expansion process is reduced due to the larger water vapor mass fraction (see Fig. 8 and Fig. 10).

Similar to the intercooled process, the compression ratio at which humidification is introduced has been varied to assess its impact on process efficiency. For both turbine inlet temperatures, best performance is achieved when diabatic cooling is introduced at N = 0.7 – 0.8. In Fig. 6 and Fig. 7, only the results obtained for N = 0.8 are shown. For a turbine inlet temperature of 900°C, the overall efficiency reaches 37.17 %, which means only a slight increase compared to conventional intercooling, yet at even further elevated turbine pressure ratios of $\pi_T = 4.5 \sim 5$.

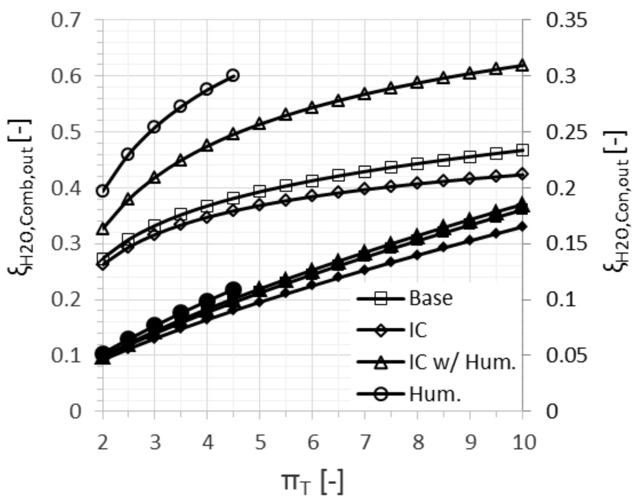

Fig. 8: Water vapor mass fraction at the combustor and condenser outlet at 1500°C TIT

At $\pi_T = 3.5$ (the best point for intercooling), the efficiencies are almost identical to those of conventional intercooling (36.72 % vs. 36.82 %). For the higher turbine inlet temperature of 1500°C, the peak efficiency is not reached up to the maximum turbine pressure ratio used. A significant increase of efficiency compared to the other cases investigated so far can be seen at higher pressure ratios, reaching values exceeding 52 %. However, for the more realistic cases with lower pressure ratios of $\pi_T < 5$, the computed efficiency for evaporation intercooling (45.46 %) is again very close to that obtained for conventional intercooling (45.07 %). Generally, the specific work output per kg of helium is further increased due to the additional water vapor mass flow. From Fig. 8 it is evident that for pressure ratios of $\pi_T > 4.5$, the water vapor mass fraction at the combustor outlet actually exceeds

50 % (i.e. the turbine mass flow is more than doubled compared to the base case) and becomes the main component of the working fluid within the turbine for this case.

Humidification between compressor and recuperator

As a final process variation, humidification between compressor and recuperator is studied. With this method, the overall mass flow is increased after compression, yielding a relative increase of turbine specific work. At the same time, diabatic cooling enhances heat exchange in the recuperator.

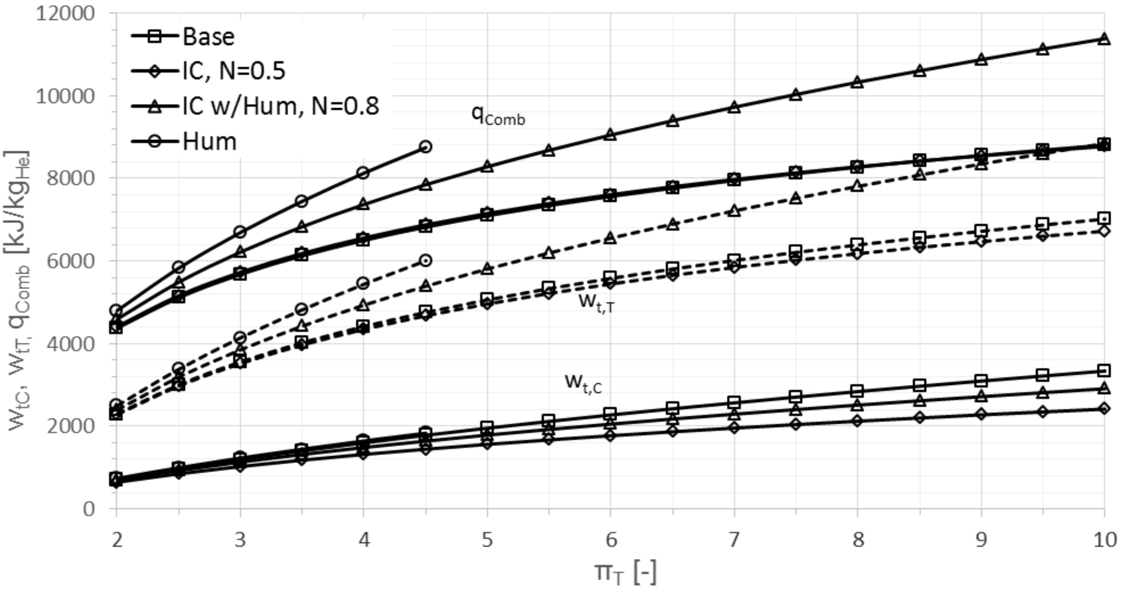

Fig. 9: Specific compression work, turbine work and combustor heat input for all processes at a turbine inlet temperature of 1500°C

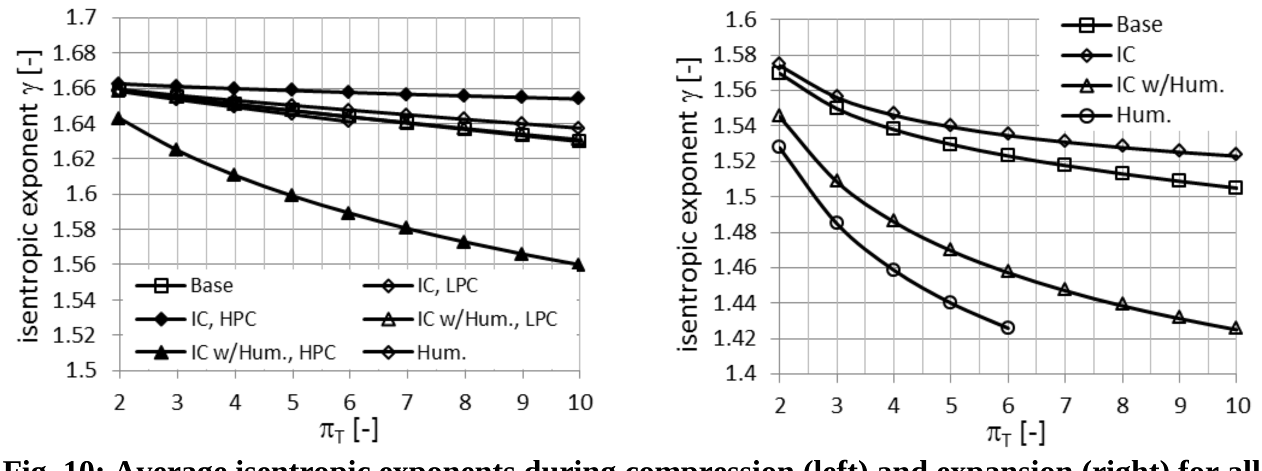

Fig. 10: Average isentropic exponents during compression (left) and expansion (right) for all processes at a turbine inlet temperature of 1500°C

Both positive effects are actually outweighed by the change of fluid properties. A high isentropic exponent close to that of pure helium is prevalent during compression as presented in Fig. 10, resulting in a large temperature increase. Consequently the specific compression work for the process with humidification is almost identical to that for the base case, which is evident from Fig. 9. On the other hand the increased mass fraction of water vapor causes a reduction of the isentropic exponent, thus yielding a reduction of enthalpy change during expansion compared to the compression process. The increased turbine mass flow partly compensates for this deficit, as it leads to a strong increase of turbine specific work, but at the same time the heat addition in the combustor increases accordingly.

For the high turbine inlet temperature case, the efficiencies obtained for this process variation are in the same range as those of the process with diabatic intercooling, yet at higher specific work output. At a TIT of 900°C, the efficiencies obtained are lower than for the diabatic cooling case, as can be seen from Fig. 6.

In order to study the impact of water temperature at humidification on process efficiency, temperatures of 100°C and 200°C have been used. An increase of the water temperature at injection leads to an increase of efficiency, especially for the lower turbine inlet temperature. The results shown here are for the higher water temperature. At turbine pressure ratios higher than $\pi_T = 4.5$ however, condensation occurs in the economizer used to pre-heat the water for injection. As the computations are terminated in this case, the peak efficiency to be expected cannot be determined from the data available. From the curves in Fig. 6 and Fig. 7, it can be concluded that the peak efficiency of the process with humidification will actually be higher than for the diabatic intercooling.

CONCLUSIONS

In order to assess the feasibility of a completely emission-free gas turbine power plant, various configurations of a closed-cycle process using a mixture of helium and water vapor as working fluid and stoichiometric combustion of hydrogen and oxygen have been modeled. With this configuration, the problem of the low allowable turbine inlet temperature for closed-cycle gas turbine plants, being their inherent disadvantage, could be tackled. The performance of the various components has been chosen according to the design data of a power plant operated between 1974 and 1988. The results show that already the basic Brayton-cycle with recuperation yields efficiencies only slightly inferior to those obtained for recent state-of-the-art air-breathing gas turbines, but at considerably increased specific work output. With regard to possible leakage problems, a system pressure level of 10 bar has been used, despite the fact that higher pressures would result in better performance. The introduction of intercooling is beneficial both in terms of process efficiency and specific work output.

Using humidification in the course of intercooling yields a further boost of specific work output due to the increase of turbine mass flow. At a low turbine inlet temperature of 900°C, the impact on efficiency is negligible, while at a high turbine inlet temperature a significant improvement can be achieved, but only for higher turbine pressure ratios. The peak efficiency was not determined for this case; values in excess of 52 % are reached for pressure ratios around 10, which is deemed to be very challenging for helium compression based on turbomachinery, even though evaporation intercooling positively affects the specific heat capacity of the gas mixture because of the increasing mass fraction of water vapor. In general, the addition of water vapor mainly affects the turbine flow, resulting in a lower isentropic exponent compared to the compression process, thus mitigating the beneficial impact of the helium gas properties. For the parameters studied in the present work, humidification between compressor and recuperator yields almost the same results as evaporative intercooling.

Especially at the higher temperature level, all process modifications considered yield efficiencies above those of the standard air-breathing cycles considered (see Fig. 6).

Further studies with steam generation downstream of the turbine and injection upstream of the combustor have been performed, the results of which indicate further substantial improvements of cycle performance. These results will be published in the near future. Moreover, the modeling will be extended to processes using pure water vapor as working fluid, similar to the cycles already investigated by Jericha (1987) in order to compare the performance of both approaches.

REFERENCES

Bammert, K., Krey, G., & Krapp, R. (1974). *Operation and Control of the 50-Mw Closed-Cycle Helium Turbine Oberhausen.* In ASME 1974 International Gas Turbine Conference and Products Show. American Society of Mechanical Engineers.

Boyce, M. P. (2011). *Gas turbine engineering handbook*, 4th ed., Elsevier.

Frutschi, H. U. (2005). *Closed-Cycle Gas Turbines - Operating Experience and Future Potential.* American Society of Mechanical Engineers, New York.

Jericha, H. (1987). *Efficient steam cycles with internal combustion of hydrogen and stoichiometric oxygen for turbines and piston engines*. International journal of hydrogen energy, 12(5), 345-354.

McBride, G. (1993). *Coefficients for Calculating Thermodynamic and Transport Properties of Individual Species.* NASA - National Aeronautics and Space Administration, Cleveland (Ohio).

McCarty, R. D. (1973). *Thermodynamic Properties of Helium4 form 2 to 1500 K at Pressure to 10^8 Pa.* American Institute of Physics, Boulder (Colorado)

Teichmann, D., Arlt, W., Wasserscheid, P., & Freymann, R. (2011). *A future energy supply based on liquid organic hydrogen carriers (LOHC)*. Energy & Environmental Science, 4(8), 2767-2773.

VDI, Verein Deutscher Ingenieure (2006). *VDI-Wärmeatlas.* Springer Verlag, Berlin, Heidelberg

Wachter, M. (2018). *Modeling of a Thermodynamic Cycle Process with Stochiometric Combustion of Hydrogen and Oxygen in Helium*. MSc-Thesis, University of Stuttgart (in German language)

Wagner W. (1973). *New vapour pressure measurements for argon and nitrogen and an new method for establishing rational vapour pressure equations.* Cryogenics, 13(8), 470-482.

Yan, X., Takizuka, T., Kunitomi, K., Itaka, H., & Takahashi, K. (2008). *Aerodynamic design, model test, and CFD analysis for a multistage axial helium compressor*. Journal of Turbomachinery, 130(3), 031018.